Journal of Biomolecular NMR, 9 (1997) 47–54
ESCOM

J-Bio NMR 410

Three-dimensional heteronuclear NMR techniques for assignment and conformational analysis using exchangeable protons in uniformly ^{13}C-enriched oligosaccharides

R. Harris, T.J. Rutherford, M.J. Milton and S.W. Homans*

Centre for Biomolecular Sciences, The Purdie Building, University of St. Andrews, St. Andrews KY16 9ST, U.K.

Received 20 May 1996
Accepted 18 October 1996

Keywords: Oligosaccharide; 3D heteronuclear NMR; *N*-Acetyllactosamine

Summary

We present heteronuclear three-dimensional gradient-NMR techniques for the resonance assignment of exchangeable (-OH and -NH) protons in uniformly ^{13}C isotopically enriched oligosaccharides and for the measurement of ^{1}H-^{1}H nuclear Overhauser enhancements involving these protons. These techniques are derived from conventional HOHAHA-HSQC and NOESY(ROESY)-HSQC experiments, and are illustrated in application to a sample of uniformly ^{13}C-enriched Galβ1-4GlcNAc, and demonstrate that a total of 35 ROEs involving exchangeable protons can be detected and assigned. We present a quantitative analysis of these ROEs that can only be accommodated in a model of the solution behaviour of the oligosaccharide that involves considerable internal motion.

Introduction

The determination of the three-dimensional structure of oligosaccharides in solution by NMR relies primarily on distance and angular constraints between contiguous monosaccharide units, derived from ^{1}H-^{1}H nuclear Overhauser enhancements (NOEs) and three-bond ^{13}C-^{1}H heteronuclear coupling constant measurements, respectively (reviewed in Homans (1994) and Van Halbeek (1994)). Unfortunately, the number of such restraints is very limited; at most three trans-glycosidic NOEs are generally observed, which together with the two heteronuclear coupling constants about the glycosidic torsion angles gives rise to a maximum of five restraints per residue. It can readily be shown that this is insufficient to distinguish between a model involving complete rigidity about the glycosidic linkage and a model involving substantial torsional fluctuation (Rutherford et al., 1993), and a larger number of conformational restraints is clearly required in order to characterise the solution behaviour with any degree of fidelity. A significant advance in this regard has been the work of Poppe and Van Halbeek, who have demonstrated that it is possible to observe the exchangeable (-OH and -NH) proton resonances of oligosaccharides in acetone/H_2O (Poppe and Van Halbeek, 1991) or in supercooled H_2O solution (Poppe and Van Halbeek, 1994). The rate of exchange at these temperatures (~255 K) is sufficiently slow that narrow line widths are obtained, thus allowing a straightforward assignment of these resonances and the measurement of NOEs to and from them. In this manner, the number of usable conformational restraints is substantially increased (Adams and Lerner, 1992a; Poppe et al., 1992).

In the present work, we describe gradient heteronuclear single-quantum correlation (HSQC) based techniques for the resonance assignment of exchangeable protons in uniformly ^{13}C-enriched oligosaccharides, and for the measurement of NOEs/ROEs involving these protons. These techniques offer substantial advantages over conventional homonuclear methods utilising 1-1 echo-type solvent suppression (Sklenář and Bax, 1987) in that they offer a very high degree of solvent suppression without phase distortions, and preserve the full intensity of resonances which appear at or near the solvent resonance frequency. Moreover, as three-dimensional ^{13}C-edited techniques, they overcome to a large extent the severe resonance

*To whom correspondence should be addressed.

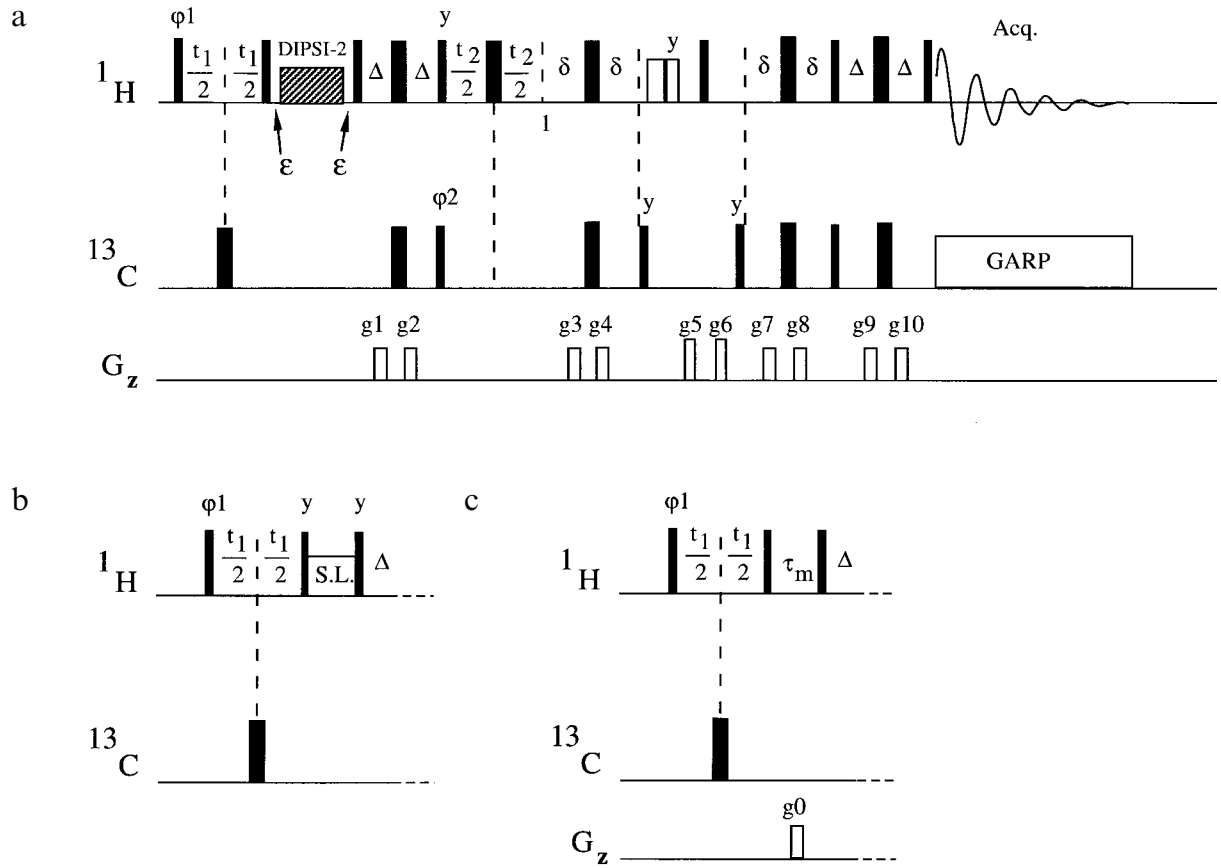

Fig. 1. Pulse sequences for (a) gd-HOHAHA-HSQC, (b) gd-ROESY-HSQC and (c) gd-NOESY-HSQC techniques described in the text. In (b) and (c), only the first part of the pulse sequence is shown; the remainder is identical to (a). Narrow bars indicate 90° pulses and wide bars indicate 180° pulses. Pulse phases are along the x-axis unless indicated otherwise. The elements of each sequence as far as point 1 are essentially derived from the HSQC analogues of their HMQC counterparts (Marion et al., 1989), followed by ^{13}C refocusing periods, solvent suppression, ^{13}C refocusing and reverse INEPT transfer to the directly attached proton. The spin-lock period in sequence (b) is of the offset-compensated type (Griesinger and Ernst, 1987) to remove the offset dependence of the intensity of the ROE. The delay Δ is set to $1/4J_{CH}$, 1.65 ms in practice, and $\delta = \Delta/2$ to ensure efficient transfer for both methylene and methine protons, or to $\delta = \Delta$ to suppress signals corresponding to methylene protons in F2. The delay $\varepsilon = 200$ μs. The proton purge pulse pair (open bars) comprises 10 kHz x and y pulses of durations 7 ms and 4.3 ms, respectively. The gradient durations and strengths are as follows: g0 = 2 ms, 8 G/cm; g1 = g2 = g9 = g10 = 1 ms, 8 G/cm; g3 = g4 = g7 = g8 = 0.5 ms, 8 G/cm; g5 = 7 ms, 12 G/cm; g6 = 4.4 ms, 12 G/cm. Phase cycling for all the experiments is as follows: $\phi1 = -x,x$, $\phi2 = x,x,-x,-x$, acq. = x,–x,–x,x. These phases are incremented by 90° in the normal manner for quadrature detection in the F1 and F2 dimensions.

overlap of nonexchangeable protons, a problem which plagues the vast majority of homonuclear NMR measurements on oligosaccharides. While this is not the first demonstration of gradient techniques for recording spectra of ^{13}C-labelled macromolecules (Kay et al., 1993; Muhandiram et al., 1993), the techniques described here offer particular advantages in application to carbohydrates.

Methods

NMR techniques

The pulse sequences for the techniques which we propose are illustrated in Fig. 1. Each sequence is essentially identical to conventional HOHAHA-HSQC (Fig. 1a), ROESY-HSQC (Fig. 1b) and NOESY-HSQC (Fig. 1c) as far as point 1, and magnetisation subsequently follows a pathway which is common to all three sequences. Transverse ^{13}C magnetisation ($2I_zS_y$) which is antiphase with respect to the attached proton at point 1 is refocused during the following interval 2δ, whose length is chosen to ensure refocusing of magnetisation from both methylene (C-6) and methine (C-1–C-5) carbons. In-phase carbon magnetisation (S_x) is then rotated into the z-axis by the first 90° ^{13}C pulse of phase y. During the time that the carbon magnetisation is along the z-axis, solvent suppression takes place using a proton purge pulse pair which dephases the solvent signal due to the inhomogeneity of the B_1 field, together with a B_0 field gradient pulse g5, as originally described by Kay et al. (1993). Residual solvent magnetisation which is along the z-axis and unaffected by g5 is rotated into the transverse plane by the 90° ^1H pulse following the purge pulse pair, and is then dephased by g6. Longitudinal ^{13}C magnetisation is then rotated into the transverse plane by the second 90° ^{13}C pulse

of phase y, followed by a dephasing period 2δ and finally reverse INEPT transfer to the directly attached proton.

Molecular modelling

Molecular dynamics (MD) simulations and grid search calculations were performed as described (Homans, 1990; Rutherford and Homans, 1994). Theoretical ROE intensities were computed from MD simulations using the in-house written software package MDNOE. This package incorporates a full relaxation matrix approach including a formalism appropriate for the computation of NOE and ROE data due to fluctuating internuclear distances arising from internal motions which are fast with respect to the rate of molecular tumbling (Tropp, 1980; Homans and Forster, 1992). Restraints were incorporated in MD simulations as biharmonic functions where the measured ROE is interpreted either in terms of a fixed distance, or alternatively in a semiquantitative manner as described (Rutherford and Homans, 1994). In the case of ROEs to hydroxymethyl protons, the latter were treated as a pseudoatom whose coordinates are the arithmetic average of the coordinates of these protons. The torsion angles φ and ψ are defined as H-1–C-1–O-1–C-4' and C-1–O-1–C-4'–H-4', respectively, where C-4' and H-4' refer to the GlcNAc residue.

Experimental

Chemoenzymatic synthesis of [U-^{13}C]-Galβ1-4GlcNAc

Uniformly ^{13}C-enriched Galβ1-4GlcNAc (LacNAc) was prepared using chemoenzymatic methods with [U-^{13}C]-GlcNAc as acceptor. Since isotopically ^{13}C-enriched GlcNAc is not commercially available to our knowledge, it was prepared by enzymatic biotransformations from [U-^{13}C]-glucose as follows. [U-^{13}C]-D-glucose (100 mg), ATP (250 mg) and L-glutamine (70 mg) were suspended in 5 ml of 50 mM Tris-HCl, pH 7.4 containing 200 mM $MgCl_2$. The pH of the reaction mixture was readjusted after the addition of ATP with 2 M NaOH, followed by the addition of hexokinase (E.C. 2.7.1.1) (10 U), phosphoglucose isomerase (E.C. 5.3.1.9) (50 U) and glucosamine synthetase (E.C. 2.1.1.6) (a generous gift from Prof. B. Badet, ENSCP, Paris) (4 U). The reaction was left to incubate for 18 h, giving [U-^{13}C]-glucosamine-6-phosphate as the principal product. The reaction mixture was adjusted to pH 9.6 with 1 M NaOH. Alkaline phosphatase (E.C. 3.1.3.1) (100 U) was added and the reaction was incubated for 5 h. The synthesis of [U-^{13}C]-D-glucosamine was confirmed by ^{1}H NMR of the crude reaction mixture. Solid $NaHCO_3$ was added to the [U-^{13}C]-D-glucosamine reaction mixture until a saturated solution was achieved, followed by the addition of 250 µl of acetic anhydride. Additional aliquots of acetic anhydride were added in 15 min intervals until all the $NaHCO_3$ had reacted. Partial purification was achieved by loading the reaction mixture to a mixed-bed column (Dowex AG50 X12 over Dowex AG3 X4) and washing through with five column volumes of deionised water. Additional purification of ^{13}C *N*-acetyl-D-glucosamine was achieved by BioGel P4 gel permeation chromatography (117 × 1.5 cm) with water as the eluant.

The disaccharide Galβ1-4GlcNAc was obtained in uniformly ^{13}C-enriched form by the enzymatic addition of [U-^{13}C]-galactose (a generous gift of Martek Biosciences, Columbia, MD, U.S.A.) to [U-^{13}C]-GlcNAc in a biotransformation involving bovine galactosyltransferase as described (Gilhespy-Muskett et al., 1994). The overall yield was ~50%.

Sample preparation

Samples were prepared by dissolution of [U-^{13}C]-Galβ1-4GlcNAc (19 mg) in 750 µl 85%/15% v/v $H_2O/(CD_3)_2CO$, pH 6.8, followed by degassing by sonication.

NMR experiments

All NMR data were acquired at 500 MHz at a probe temperature of 256 K using dry nitrogen as the cooling gas and isopropanol/solid CO_2 as the coolant, on a single sample of [U-^{13}C]-Galβ1-4GlcNAc in 85% H_2O/15% $(CD_3)_2CO$. Two-dimensional gradient-HOHAHA-HSQC spectra (gd-HOHAHA-HSQC) were acquired with spectral widths of 1000 Hz in F2 and 3450 Hz in F1, with 1024 and 256 complex points, respectively. Sixteen transients were acquired per t_1 increment, giving a total acquisition time of ~4 h. The spin-lock time was 35 ms, using DIPSI-2 with a 7.6 kHz rf field whose carrier was located at 5.3 ppm. Immediately prior to acquisition, the carrier was shifted to 4.35 ppm in order to reduce the spectral width in the F3 dimension. Prior to two-dimensional Fourier transformation, data were apodised with cosine-bell functions, followed by zero-filling once in each dimension. Two-dimensional gradient-ROESY-HSQC spectra (gd-ROESY-HSQC) were acquired under otherwise identical conditions, except that the spin-lock time was 100 ms using a weak (~3 kHz) continuous-wave rf field. Three-dimensional gd-ROESY-HSQC spectra were acquired with spectral widths of 1000 Hz in F3 (^{1}H), 3450 Hz in F1 (^{1}H) and 3600 Hz in F2 (^{13}C) and with 512, 128 and 32 complex points, respectively. Four transients were acquired per increment, giving a total acquisition time of ~24 h. Prior to three-dimensional Fourier transformation, data were apodised with cosine-bell functions, followed by zero-filling once in each dimension. The recycle delay in all experiments was 1 s.

The rotational correlation time of the disaccharide was measured by ^{13}C T_1 relaxation time measurements and was also calibrated independently from diagonal versus cross-peak volumes for fixed internuclear distances using a full relaxation matrix analysis. The value obtained (2.5 ± 0.2 ns) reflects the high viscosity of the disaccharide solution at 256 K.

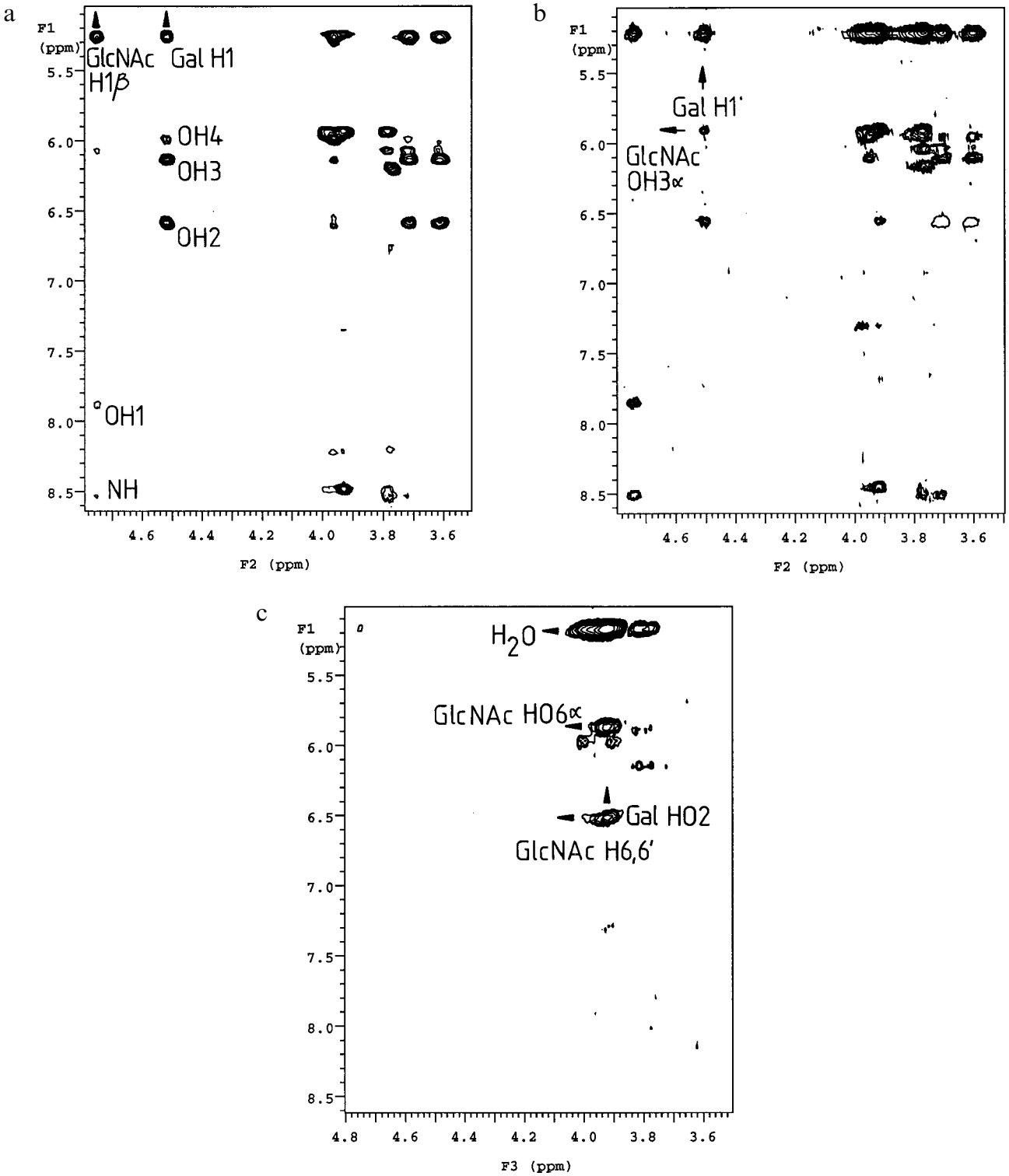

Fig. 2. (a) Region of the two-dimensional gd-HOHAHA-HSQC spectrum (mixing time = 35 ms) of [U-^{13}C]-Galβ1-4GlcNAc showing through-bond connectivities from nonexchangeable protons to hydroxyl and amide protons. Selected cross peaks are assigned as shown. The delay $\delta = \Delta$ to suppress signals corresponding to methylene protons in F2. (b) Region of the two-dimensional gd-ROESY-HSQC spectrum (mixing time = 100 ms) showing through-space connectivities to exchangeable protons. The delay $\delta = \Delta/2$ to ensure efficient transfer for both methylene and methine protons. A typical trans-glycosidic connectivity is shown. In addition to through-space connectivities, two through-bond connectivities are observable from Gal H-2 and Gal H-3 to Gal OH-2 (negative intensities, plotted as single contours). These derive from HOHAHA-type transfer which is efficient for these protons despite the weak continuous-wave field due to the choice of resonance offset. Spectra in (a) and (b) were acquired with the three-dimensional sequences shown in Fig. 1 by setting delay t_2 to zero. (c) Plane from the three-dimensional gd-ROESY-HSQC spectrum at the ^{13}C resonance frequency of GlcNAcα/β C-6 (identical shift for each anomer) showing the much improved resolution in comparison with (b). The delay $\delta = \Delta/2$. Cross peaks are assigned as shown.

TABLE 1
PROTON RESONANCE ASSIGNMENTS AND EXCHANGE RATES FOR EXCHANGEABLE PROTONS IN UNIFORMLY ^{13}C-ENRICHED Galβ1-4GlcNAc IN $H_2O/(CD_3)_2CO$ AT 256 K

Proton	Shift (ppm)	Exchange rate K (s^{-1})
Galactose		
OH-2	6.54	9.7
OH-3	6.09	15.1
OH-4	5.94	10.7
OH-6	6.15	15.0[a]
GlcNAcα		
OH-1	7.28	12.5
NH-2	8.48	–
OH-3	5.89	8.9
OH-6	5.89	15.0[a]
GlcNAcβ		
OH-1	7.83	15.1
NH-2	8.43	–
OH-3	6.03	6.5
OH-6	5.99	15.0[a]

Chemical shifts are referenced indirectly to 3-(trimethylsilyl)propanesulphonic acid sodium salt, δ = 0 at 256 K.
[a] Approximate value due to low signal intensity.

Results

Resonance assignment

The two-dimensional gd-HOHAHA-HSQC spectrum of [U-^{13}C]-Galβ1-4GlcNAc at 256 K is illustrated in Fig. 2a, showing the region in F1 downfield of the H_2O resonance corresponding to exchangeable protons. At this mixing time (35 ms), a number of cross peaks corresponding to single-step and relayed ^{1}H-^{1}H coherence transfers are observable. From the intensities of these, combined with additional experiments at shorter mixing times (data not shown), the resonance assignment of hydroxyl and amide protons is straightforward using the assignments for nonexchangeable protons as a basis. A selection of assignments for exchangeable protons is shown in Fig. 2a, and the remainder are compiled in Table 1. An interesting feature of the data in Fig. 2 is the presence of cross peaks from nonexchangeable protons to the solvent water resonance at F1 ~ 5.25 ppm, which derive from a slow exchange between the hydroxyl and amide protons and the bulk solvent. The excellent solvent suppression obtained with the pulse sequences in Fig. 1 allows such cross peaks to be readily observed. Also of note is the absence of phase distortions in the spectrum, and the appearance of resonances close to the water at full intensity due to the absence of frequency-dependent excitation profiles obtained with 'jump-return'-type techniques (Poppe and Van Halbeek, 1991,1994; Poppe et al., 1992).

A notable feature of the HOHAHA-HSQC sequence, in common with the other sequences in Fig. 1, is the ability to achieve a degree of spectral editing; by setting the delay δ to Δ (as in Fig. 2a) rather than Δ/2 (as in Figs. 2b and c), all signals corresponding to methylene protons are suppressed in F2. In practice, we find this feature to be very useful not only for editing connectivities from the H-6 protons to exchangeable protons, but also for editing cross peaks in the nonexchangeable region of the spectrum, which substantially reduces the resonance overlap problem in this region.

Structural restraints involving hydroxyl protons

Figure 2b shows the two-dimensional gd-ROESY-HSQC spectrum of [U-^{13}C]-Galβ1-4GlcNAc at 256 K obtained under otherwise identical conditions to those described above. A substantial number of cross peaks are observed to both hydroxyl and amide protons, together with intense correlations to the solvent water resonance. While several of these cross peaks can immediately be assigned by inspection, resonance overlap in the region F1 ~ 6.0 ppm is sufficiently severe to prevent the unambiguous assignment of all cross peaks. This problem is readily overcome by editing the spectrum in a third ^{13}C frequency dimension in the conventional manner (Kay et al., 1989). An example is shown in Fig. 2c, which illustrates an F1/F3 slice at the ^{13}C resonance frequency of GlcNAcα/β C-6 (identical shift for each anomer). Apart from the intraresidue connectivities between the H-6 protons of GlcNAcα and GlcNAcβ and the corresponding OH-6 resonances, an interresidue connectivity can readily be detected between the H-6 protons of each anomer and Gal OH-2. The complete set of ROE connectivities observed and assigned to exchangeable protons is given in Table 2.

TABLE 2
ROE CONNECTIVITIES TO EXCHANGEABLE PROTONS IN Galβ1-4GlcNAc

Proton	ROE connectivities
Galactose	
H-1	OH-2, GlcNAcα/β OH-3 GlcNAcα/β OH-6
H-2	OH-2, OH-3, OH-4
H-3	OH-2, OH-3, OH-4
H-4	OH-3, OH-4
H-5	OH-3, OH-4
H-6/6'	OH-4, OH-6
GlcNAcα	
H-1	OH-1, NH-2
H-2	NH-2, OH-3
H-3	NH-2, OH-3
H-4	OH-1, NH-2, OH-3
H-5	OH-1, OH-6
H-6	OH-6, Gal OH-2
GlcNAcβ	
H-1	OH-1, NH-2
H-2	NH-2, OH-3
H-4	OH-3
H-6	OH-6, Gal OH-2

TABLE 3
EXPERIMENTAL ROEs INVOLVING EXCHANGEABLE PROTONS COMPARED WITH THEORETICAL VALUES DERIVED FROM TWO 500 ps RESTRAINED MD SIMULATIONS IN VACUO FOR Galβ1-4GlcNAc

ROE connectivity	ROE intensity (%)	
	Experimental[a]	Theoretical
(a)		
H-1–OH-3'	0.7	0.1
H-1–OH-6'	0.5[b]	1.0
OH-2–H-6'*[c]	2.0	1.0
(b)		
H-1–OH-3'	0.7	1.2
H-1–OH-6'	0.5[b]	0.2
OH-2–H-6'*[c]	2.0	2.3

(a) Restraints: H-1–H-4': 2.34 Å < r < 2.54 Å; H-1–H-6': 2.92 Å < r < 3.12 Å; force constant = 10 kcal/Å^2.
(b) Restraints: H-1–H-4': 1.8 Å < r < 2.7 Å; H-1–H-6': 1.8 Å < r < 5.0 Å; force constant = 10 kcal/Å^2.
[a] Experimental values (±10%) expressed as the sum of intensities of α and β anomers.
[b] Estimated error ±25% due to low cross-peak intensity.
[c] Theoretical value computed as the sum of the ROEs to each hydroxymethyl proton. *: treated as a pseudoatom.

A similar series of correlations to those given in Table 2 is observed in the gd-NOESY-HSQC spectrum of the disaccharide (not shown). At 256 K the rotational tumbling time of a disaccharide is such that the observed NOEs are weak and negative (i.e. cross peaks have the same sign as diagonal peaks). Consequently, the gd-ROESY-HSQC technique is the method of choice for small carbohydrates, whereas the gd-NOESY-HSQC technique will be of more value for larger oligosaccharides.

Quantitation of ROE data involving exchangeable protons

The extraction of quantitative distance information from cross-peak intensities involving exchangeable protons is not straightforward. First, as discussed by James and co-workers (Liu et al., 1993), a loss of cross-peak intensity arises from the exchange of magnetisation with solvent water. This is effectively a leakage process which affects only the diagonal elements of the relaxation matrix, and can be accounted for in a full relaxation matrix calculation of the ROESY or NOESY intensities provided the exchange rates are known. The latter can be measured in a straightforward manner using, for example, the approach described by Adams and Lerner (1992b), and these values are included in Table 1. A second problem concerns the extent of saturation of the water magnetisation. If the water magnetisation is saturated prior to acquisition, substantial saturation transfer can occur from the bulk solvent (which is in vast excess) to the solute during the acquisition period and relaxation delay, and can result in a substantial reduction in the resonance intensity of exchangeable protons (Grzesiek and Bax, 1993; Li and Montelione, 1993; Stonehouse et al., 1994). An alternative is to employ selective 'flip-back' pulses (Grzesiek and Bax, 1993) or a judicious choice of phase cycling (Mori et al., 1995) together with tailored excitation techniques such as WATERGATE (Sklenář et al., 1993), which ensure that the bulk of the water magnetisation is returned along the +z-axis immediately prior to acquisition. Unfortunately, none of these techniques is of value in the present application, since they all require selective excitation (or selective nonexcitation) at the water resonance frequency. Unlike the amide protons of proteins which resonate well downfield of the water resonance, the anomeric protons of oligosaccharides resonate at or close to the water resonance frequency, and would also be effectively attenuated using these techniques. While the sequences described in the present study would therefore appear to be inappropriate for quantitative analysis since they involve deliberate saturation of the water prior to acquisition, in practice we find that negligible attenuation of cross-peak intensities occurs due to rapid recovery of the water magnetisation under the experimental conditions employed. The longitudinal relaxation rate of the water magnetisation can conveniently be measured using a simple modification of the sequence in Fig. 1b where the final π/2 proton pulse was followed by a variable delay and an additional π/2 proton read pulse to monitor the recovery of water magnetisation, which is shown in Fig. 3.

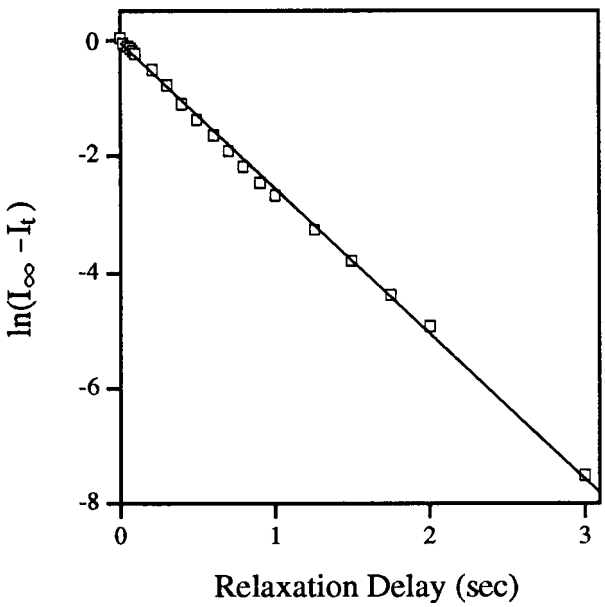

Fig. 3. Plot of recovery of water magnetisation during the acquisition period and relaxation delay of the pulse sequence shown in Fig. 1b. The recovery of the water magnetisation was measured using a simple modification of the sequence in Fig. 1b where the final π/2 proton pulse was followed by a variable delay and an additional π/2 proton read pulse to monitor the z component of the water magnetisation. The measured longitudinal relaxation rate of the water magnetisation at 256 K is 2.5 s^{-1}.

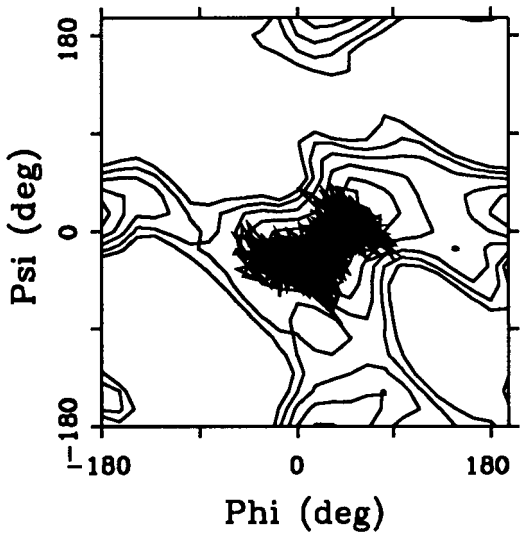

Fig. 4. Instantaneous values of the glycosidic torsion angles ϕ and ψ over the 500 ps restrained MD simulation in vacuo for Galβ1-4GlcNAc. Biharmonic restraints were applied with a force constant of 10 kcal/Å^2 and with bounds as follows: H-1–H-4': 1.8 Å < r < 2.7 Å; H-1–H-6': 1.8 Å < r < 5.0 Å. Contours derived from a grid search calculation about ϕ and ψ are plotted at 1.0, 2.0, 3.0, 4.0 and 5.0 kcal/mol above the global minimum.

Simulations of the recovery of the hydroxyl proton magnetisation using a simple two-spin system undergoing two-site exchange (Stonehouse, 1994) and with the measured T_1 of water (400 ms) show that the recovery of the hydroxyl magnetisation is complete to ~90% after 1 s, for values of the hydroxyl proton exchange rate K of $5 < K < 25\ s^{-1}$ and for the hydroxyl proton longitudinal relaxation rate R_I of $0.07 < R_I < 7\ s^{-1}$. This indicates that no correction of cross-peak intensities is required for a combined acquisition time and relaxation delay greater than 1 s for all values of the exchange rate and hydroxyl proton T_1 that are likely to be encountered in practice. The essential independence of the recovery with respect to R_I is very useful in view of the difficulty in obtaining an accurate value for this parameter, and arises from the rapid recovery of the solvent magnetisation at the low temperatures necessary for the observation of exchangeable protons in oligosaccharides.

Structural implications of ROE data for exchangeable protons

Only two trans-glycosidic NOEs are observed in Galβ1-4GlcNAc that do not involve exchangeable protons. As in previous studies (Rutherford et al., 1993), we find that these restraints are consistent with models for the solution behaviour of the glycan involving a single conformation or, alternatively, multiple conformations. As discussed in detail elsewhere (Rutherford et al., 1993), this arises from the paucity of restraints across the glycosidic linkage. In order to assess the impact of the additional restraints obtained here, it is necessary to take account of the very rapid (picosecond) motional averaging of the hydroxyl groups about their respective C-O bond, which gives rise to fluctuating internuclear distances. A convenient method for achieving this is by simulation of the MD trajectory of the glycan in vacuo for a period of time which is much longer than the time scale of the internal motions. In the present study, a 500 ps restrained MD simulation was computed, with restraints derived from the trans-glycosidic NOEs involving nonexchangeable protons. These restraints were applied as 'fixed' distances, corresponding with the 'single conformation' model involving limited torsional fluctuations about the glycosidic linkage. The time-averaged trans-glycosidic NOEs involving exchangeable protons were then calculated over the time course of the simulation, using a full relaxation matrix analysis including a formalism appropriate for fluctuating internuclear distances due to internal motions which are rapid with respect to overall isotropic tumbling (Tropp, 1980; Homans and Forster, 1992). One of these NOEs involves GlcNAc OH-6, which forms part of the pendant hydroxymethyl group whose internal rotation about the C-5–C-6 bond is slow with respect to overall tumbling. It was therefore necessary to compute two MD simulations with the dihedral angle ω about the C-5–C-6 bond weakly restrained to the two values (180° (66%) and –60° (34%)) which were observed to exist in the disaccharide on the basis of homonuclear spin-coupling constant measurements. A weighted average was then taken over the two simulations. The results for the relevant trans-glycosidic NOEs involving exchangeable protons are given in Table 3, where it is seen in particular that the NOE between Gal H-1 and GlcNAc OH-3 is severely underestimated in these simulations. This immediately suggests that substantial torsional fluctuations exist in the disaccharide in free solution, and indeed the experimental NOEs compare more favourably with predicted values when the restraint bounds corresponding to the two original NOEs are relaxed (Table 3). The resulting torsional fluctuations about ϕ and ψ lie within the global minimum energy region of the glycan (Fig. 4), and offer a plausible model for the dynamic behaviour of the glycan in solution.

Discussion and Conclusions

By use of the above techniques, at least 35 ROEs can be observed and assigned to hydroxyl and amide protons in Galβ1-4GlcNAc, including three trans-glycosidic connectivities. These are of crucial importance for conformational studies, since often only a single ROE(NOE) involving nonexchangeable protons is observed across the glycosidic linkage. Such NOEs tend by nature to involve protons located very close to the glycosidic linkage, and are not very sensitive to torsional fluctuations about the glycosidic linkage. By contrast, NOEs involving OH and NH protons in oligosaccharides are not necessarily proxi-

mal to the glycosidic linkage, and hence are much more sensitive to conformation. Although we have examined a simple disaccharide in the present study, sufficient additional NOEs are observed to confirm that substantial torsional fluctuations exist about the glycosidic linkage, a result that in the past has not been obvious without recourse to detailed relaxation time measurements (Rutherford et al., 1993). In more complex branched oligosaccharides, it would be anticipated that the number of interresidue connectivities involving exchangeable protons will be much higher, and therefore will be of even greater value in conformational studies.

A less obvious, but equally useful, application of the above techniques is as an aid to oligosaccharide primary sequence determination; while oligosaccharide linkage positions can be inferred from trans-glycosidic nuclear Overhauser effect measurements, the presence of an NOE from an anomeric proton to an aglyconic proton is no guarantee that the linkage site is to the respective carbon atom of the aglycon since the precise NOE connectivity observed can depend upon the local conformation. In contrast, the direct observation of hydroxyl protons, provided they can all be assigned, overcomes this problem since a hydroxyl proton obviously cannot exist at a site of O-glycosylation.

A disadvantage of the techniques described here is the requirement for isotopically ^{13}C-enriched oligosaccharides for high sensitivity. However, in common with NMR studies on other macromolecules, isotopic enrichment is of enormous value in extending the types of NMR measurements that can be undertaken. This is of particular relevance to studies on oligosaccharides where the very poor spectral dispersion in the proton dimension is a severe hindrance to structural studies. Given that it is now possible to obtain isotopically enriched oligosaccharides by the growth of bacteria (Yu et al., 1993) and parasites (Weller et al., 1994) on isotopically enriched media, and glycoproteins by overexpression in mammalian cells (Lustbader et al., 1996; Weller et al., 1996), the requirement for ^{13}C-enriched glycans is not likely to be prohibitive in the future.

Acknowledgements

This work was supported by The Wellcome Trust, Grant 040331/Z/93/Z. S.W.H. is a Lister Institute Centenary Research Fellow. The authors acknowledge valuable discussions with Drs. James Keeler and Chun-Wa Chung.

References

Adams, B. and Lerner, L. (1992a) *J. Magn. Reson.*, **96**, 604–607.
Adams, B. and Lerner, L. (1992b) *J. Am. Chem. Soc.*, **114**, 4827–4829.
Gilhespy-Muskett, A.M., Partridge, J., Jefferis, R. and Homans, S.W. (1994) *Glycobiology*, **4**, 485–489.
Griesinger, C. and Ernst, R.R. (1987) *J. Magn. Reson.*, **75**, 261–271.
Grzesiek, S. and Bax, A. (1993) *J. Am. Chem. Soc.*, **115**, 12593–12594.
Homans, S.W. (1990) *Biochemistry*, **29**, 9110–9118.
Homans, S.W. and Forster, M. (1992) *Glycobiology*, **2**, 143–151.
Homans, S.W. (1994) In *Molecular Glycobiology* (Eds., Fukuda, M. and Hindsgaul, O.), IRL Press, New York, NY, U.S.A., pp. 230–257.
Kay, L.E., Marion, D. and Bax, A. (1989) *J. Magn. Reson.*, **84**, 72–84.
Kay, L.E., Xu, G.Y., Singer, A., Muhandiram, D.R. and Forman-Kay, J.D. (1993) *J. Magn. Reson.*, **B101**, 333–337.
Li, Y.C. and Montelione, G.T. (1993) *J. Magn. Reson.*, **B101**, 315–319.
Liu, H., Kumar, A., Weisz, K., Schmitz, U., Bishop, K.D. and James, T.L. (1993) *J. Am. Chem. Soc.*, **115**, 1590–1591.
Lustbader, J.W., Birken, S., Pollak, S., Canfield, R.E., Chait, B.T., Mirza, U.A., Ramnarain, S. and Brown, J.M. (1996) *J. Biomol. NMR*, **7**, 295–304.
Marion, D., Driscoll, P.C., Kay, L.E., Wingfield, P.T., Bax, A., Gronenborn, A.M. and Clore, G.M. (1989) *Biochemistry*, **28**, 6150–6156.
Mori, S., Abeygunawardana, C., O'Neil Johnson, M. and Van Zijl, P.C.M. (1995) *J. Magn. Reson.*, **B108**, 94–98.
Muhandiram, D.R., Farrow, N.A., Xu, G.-U., Smallcombe, S.H. and Kay, L.E. (1993) *J. Magn. Reson.*, **B102**, 317–321.
Poppe, L. and Van Halbeek, H. (1991) *J. Am. Chem. Soc.*, **113**, 363–365.
Poppe, L., Stuike-Prill, R., Meyer, B. and Van Halbeek, H. (1992) *J. Biomol. NMR*, **2**, 109–136.
Poppe, L. and Van Halbeek, H. (1994) *Nat. Struct. Biol.*, **1**, 215–216.
Rutherford, T.J., Partridge, J., Weller, C.T. and Homans, S.W. (1993) *Biochemistry*, **32**, 12715–12724.
Rutherford, T.J. and Homans, S.W. (1994) *Biochemistry*, **33**, 9606–9614.
Sklenář, V. and Bax, A. (1987) *J. Magn. Reson.*, **74**, 469–479.
Sklenář, V., Piotto, M., Leppik, R. and Saudek, V. (1993) *J. Magn. Reson.*, **A102**, 241–245.
Stonehouse, J. (1994) Ph.D. Thesis, University of Cambridge, Cambridge, U.K.
Stonehouse, J., Shaw, G.L., Keeler, J. and Laue, E.D. (1994) *J. Magn. Reson.*, **A107**, 178–184.
Tropp, J. (1980) *J. Chem. Phys.*, **72**, 6035–6044.
Van Halbeek, H. (1994) *Curr. Opin. Struct. Biol.*, **4**, 697–709.
Weller, C.T., McConville, M. and Homans, S.W. (1994) *Biopolymers*, **34**, 1155–1163.
Weller, C.T., Lustbader, J., Seshadri, K., Brown, J.M., Chadwick, C.A., Kolthoff, C.E., Ramnarain, S., Pollak, S., Canfield, R. and Homans, S.W. (1996) *Biochemistry*, **35**, 8815–8823.
Yu, L., Goldman, R., Sullivan, P., Walker, G.F. and Fesik, S.W. (1993) *J. Biomol. NMR*, **3**, 429–441.